



Recharge mechanisms of deep soil water revealed by water isotopes in deep loess deposits

Wei Xiang^a, Jaivime Evaristo^{b,c}, Zhi Li^{b,*}

^a Key Laboratory of Agricultural Soil and Water Engineering in Arid and Semiarid Areas, Ministry of Education, Northwest A&F University, Yangling, Shaanxi Province 712100, China

^b College of Natural Resources and Environment, Northwest A&F University, Yangling 712100, China

^c Copernicus Institute of Sustainable Development, Utrecht University, Utrecht, The Netherlands

ARTICLE INFO

Keywords:

Deep soil
Water isotopes
Land use change
The Loess Plateau
Ecohydrology

ABSTRACT

Isotopes in soil water are useful tracers of flow and transport processes in the subsurface. The combined utility of stable (^2H , ^{18}O) and radioactive (^3H) isotopes in soil water, however, is seldom explored in vadose zone studies, particularly in identifying deep soil water recharge mechanisms (sources, fluxes, and ages). Here we show that the combined use of ^2H , ^{18}O , and ^3H can identify the sources and recharge mechanisms of water to thick deep soils of the Loess Plateau, China. We found that high soil water tritium concentrations were limited between 6 and 7 m from the surface, suggesting that soils deeper than 7 m were comprised of water older than ~50 years, while soils shallower than 6 m represented water younger than ~50 years. We also found that rainfall intensity played an important role in deep soil water recharge. Stable isotopes suggest that only a few extreme rainfall events (≥ 30 mm/day) during the rainy season infiltrated to deep soil layers, but the age of water that recharged the soils at these depths were older than ~50 years as inferred from tritium. These combined insights from stable and radioactive isotopes in soil water suggest that (1) waters in these deep soils are much older than the apple orchards that cover these landscapes, and (2) very few high-intensity rainfall events have reached the deeper parts of the soil profile since the apple orchards were established < 24 years ago. The latter is supported by our findings that deep soil water storage beneath the apple orchards was significantly reduced, presumably because of root water uptake. Our results demonstrate the combined utility of tritium and stable isotopes in identifying relative ages and mechanisms of soil water recharge, and in characterizing the possible effects of land cover on soil water movement. We anticipate broader applicability of these findings, particularly in characterizing water resources sustainability against the backdrop of changing land cover in other arid and semi-arid regions.

1. Introduction

Soils partition precipitation into different compartments of the terrestrial hydrosphere (Bowen, 2015). Environmental isotopes are a staple in terrestrial hydrosphere research because they provide information about the sources, pathways, and ages of water in catchments (McGuire and McDonnell, 2015). Such information is fundamental to attaining water resources sustainability against the backdrop of global land-use change (Evaristo and McDonnell, 2019). Notwithstanding the explosion in the number of tracer studies in soil and water resources science (Penna et al., 2018; Sprenger et al., 2016), advancing our knowledge of critical zone processes (Brantley et al., 2017; Evaristo et al., 2016) and ecohydrological dynamics (Berry et al., 2018; McCutcheon et al., 2017), the combined use of stable (^2H , ^{18}O) and radioactive (^3H) isotopic systems in hydrologic studies has been

relatively rare. This is problematic because while tritium may be useful for dating waters with ages of up to several decades in the subsurface (Li et al., 2018a; Li and Si, 2018; Morgenstern et al., 2010) and in vegetation (Zhang et al., 2017), stable water isotopes are more sensitive to evaporation and condensation (Craig, 1961; Evaristo et al., 2016). This suggests that stable water isotopes are more suitable for characterizing waters younger than a few years (Stewart et al., 2010). The difference in the ranges of temporal resolution between stable and radioactive water isotope systems suggests that one system can provide an effective constraint on the other in terms of soil water age determination and soil water recharge mechanisms.

Recent works suggest that soils may partition infiltration water into a pool that sustains transpiration and another pool that recharges groundwater reservoirs and generates streamflow (Brooks et al., 2010; Evaristo et al., 2015). Given that soil water plays an important role in

* Corresponding author.

E-mail address: lizhibox@nwfufu.edu.cn (Z. Li).

these processes, a few conceptual models have been developed to describe how soil water are recharged (Brooks, 2015; Brooks et al., 2010; Sprenger et al., 2016). However, it remains controversial (Berry et al., 2018). Therefore, identifying the recharge mechanisms (sources, pathways, fluxes, and ages) of soil water, in particular, is critical for understanding soil and hydrological processes (Brantley et al., 2017; Sprenger et al., 2016). This in turn are relevant for applications in sustainable development of soil and water resources.

While most infiltration water quickly returns to the atmosphere via evapotranspiration in shallow soils, a small fraction of water infiltrates into deep soils, and/or further recharges groundwater systems, eventually generating streamflow (Good et al., 2015). Understanding the mechanisms of deep soil water recharge is important because of a growing body of research that points to the pivotal role of deep soil water in mitigating the vulnerability of deep-rooted ecosystems to seasonal droughts and land-use change (Giardina et al., 2018; Li et al., 2019c; Nepstad et al., 1994; Rempe and Dietrich, 2018; Yang et al., 2017; Zunzunegui et al., 2018). Notwithstanding, deep soil water recharge mechanisms are poorly understood (Allen et al., 2019; Salve et al., 2012; Xu et al., 2019), especially in regions with thick vadose zones and low infiltration rates. The steady state of soil water in the deep soils tends to obscure some critical information.

China's Loess Plateau (CLP) hosts the world's deepest and largest loess deposits, with a mean thickness of 100 m and a maximum thickness of up to ~350 m (Zhu et al., 2018). Cast against the backdrop of a dry climate, groundwater extraction for irrigation is a suboptimal choice because of the deep water tables at the CLP (> 30 m) (Li et al., 2019d). This suggests that deep soil water is an important source of water, especially for deep-rooted vegetation (Shao et al., 2018b). Historically, a series of afforestation programs – overarched by the Grain-for-Green project in 1999 – have been implemented since the 1950s (Fu et al., 2017; Li et al., 2017a). While the afforestation programs have served their main goal in enhancing soil stability, there come with some unprecedented consequences. Many newly planted trees are deep-rooted (up to 23.2 m below the ground) (Li et al., 2019c; Wang et al., 2015), which reduces water storage and limits the ecological sustainability of revegetation (Feng et al., 2016; Peng and Li, 2018). Most efforts to date have focused on investigating the response of deep soil water storage to climatic, soil, vegetation, and topography at CLP (Jia et al., 2017; Li et al., 2019a; Wang et al., 2011; Yang et al., 2012). Not as much attention has been given to understand *how* and *when* deep soil water storage is recharged. Identifying the mechanisms of deep soil water recharge in the CLP, therefore, has emerged as a key research priority. While it has been demonstrated elsewhere that soil water storage is recharged mainly by precipitation in the rainy season (Brooks et al., 2010; Xu et al., 2019), the same has yet to be confirmed in this region.

In this study, we use stable water isotopic measurements together with a relatively rare record of soil water tritium concentrations in the vadose zone to interpret the recharge mechanisms of soil water in the CLP. We combine these data primarily to answer an overarching question, *what insights can be drawn from the combined use of stable and radioactive water isotopes in characterizing the sources and ages of soil water?* We leverage an experimental setting in the south of the CLP with deep vadose zones (0–20 m) and where a distinct mid-1960s tritium bomb signal is well preserved to the present day (Zhang et al., 2017).

2. Materials and methods

2.1. Study site

This study was conducted at the Changwu Agroecological Experiment Station (35.2°N, 107.8°E), located in the southern part of the Loess Plateau (Fig. 1a and b). The site is relatively flat and unirrigated. Soil is predominantly silt loam with silt content > 50% and belongs to Heilu soil (Zhu et al., 1983). The area is located in warm

temperate zone, and has a continental monsoon climate, with the long-term (1957–2018) mean annual temperature, precipitation, and potential evapotranspiration of 9.4 °C, 581 mm, and 903 mm, respectively. More than half of annual precipitation takes place between July and September (rainy season) as heavy rainfall events (Fig. 1c), sustaining the source of water for agriculture in the area. Groundwater is determined to be 84 m below the surface.

2.2. Sample collection

Precipitation samples were collected on daily basis at one site (Changwu station; Fig. 1b) for eight years (2005, 2010, and 2013–2018), and the continuous monitoring between 18 February 2013 and 16 July 2018 was presented in Fig. 2a. Rainfall water flowed directly into a bottle connected to a rainfall water funnel, and a ping pong ball was placed in the funnel to minimize evaporation (Li et al., 2017b). Each sample was stored in a 150 mL polyethylene plastic bottle and refrigerated at 4 °C before further isotope analysis. In particular, the daily-based precipitation isotope data in 2005, 2010, and 2013–2015 were obtained from literatures at the same site (Cheng et al., 2014; Li et al., 2017b). In total, 228 daily-based precipitation samples (or isotope data) were collected ($n = 50$ in the current study and $n = 178$ in literature).

Six sites were selected for this study that sampled at different time spanned between 2015 and 2018: three under long-term (> 100 years) farmlands (F1–F3), and the remaining under apple orchards (A17, A18, and A24) with the stand ages 17, 18, and 24 years, respectively (Fig. 1b; Table 1). These apple orchards were farmlands prior to land use conversion. All sites are in close proximity to one another (< 1 km), subject to the same hydrometeorological, topographical, and soil conditions. We collected soil samples by drilling into soil with a hollow-stem auger (0.04 m in diameter and 0.25 m in length). Soil cores were taken down to a depth of 20 m and subdivided into 0.2-m sampling intervals. Each soil sample was mixed well by hand and split into two parts. One part, about 40 g, was used to determine gravimetric soil water content via the oven-dry method (105 °C for 12 h). Soil water content was then converted to soil water storage using the measured bulk density (Lu et al., 2019). The other soil sample was stored in bottles, in a refrigerator at –20 °C. The bottled soil samples were then directly used for water extraction.

2.3. Isotope measurement

Soil water was extracted via the cryogenic vacuum distillation method (Orlowski et al., 2016). The extracted soil water was then stored in 25 mL glass bottles and refrigerated at 4 °C prior to stable isotope analysis. The stable isotopic compositions of soil water ($n = 226$) and precipitation ($n = 50$) were analyzed using LGR LIWA V2 isotopic liquid water analyzer (Los Gatos Research Inc., USA). Laboratory precision was 1.0‰ for $\delta^2\text{H}$ and 0.2‰ for $\delta^{18}\text{O}$. Results are expressed as δ values in per mil (‰):

$$\delta_{\text{sample}} = \frac{R_{\text{sample}}}{R_{\text{VSMOW}}} - 1 \quad (1)$$

where δ_{sample} is the isotopic composition ($\delta^2\text{H}$ or $\delta^{18}\text{O}$) of the sample, and R_{sample} and R_{VSMOW} as the ratio of $^{18}\text{O}/^{16}\text{O}$ or $^2\text{H}/^1\text{H}$ in the sample and in the Vienna Standard Mean Ocean Water (VSMOW), respectively.

In addition, we measured radioactive tritium abundance of the extracted soil water samples that under the 17-year-old apple orchard. Tritium isotope measurements were performed by mixing ~8 mL soil water with 12 mL scintillation solution (Hisafe3) in a 25 mL standard plastic bottle. After 24 h of dark adaptation, we measured the tritium activities in counts per minute, averaged over 500 min counting period using a liquid scintillation counter (Quantulus 1220, PerkinElmer, Singapore). In total of 28 soil water samples that cover soil depths between 0 and 15 m, were measured, and the result was given in

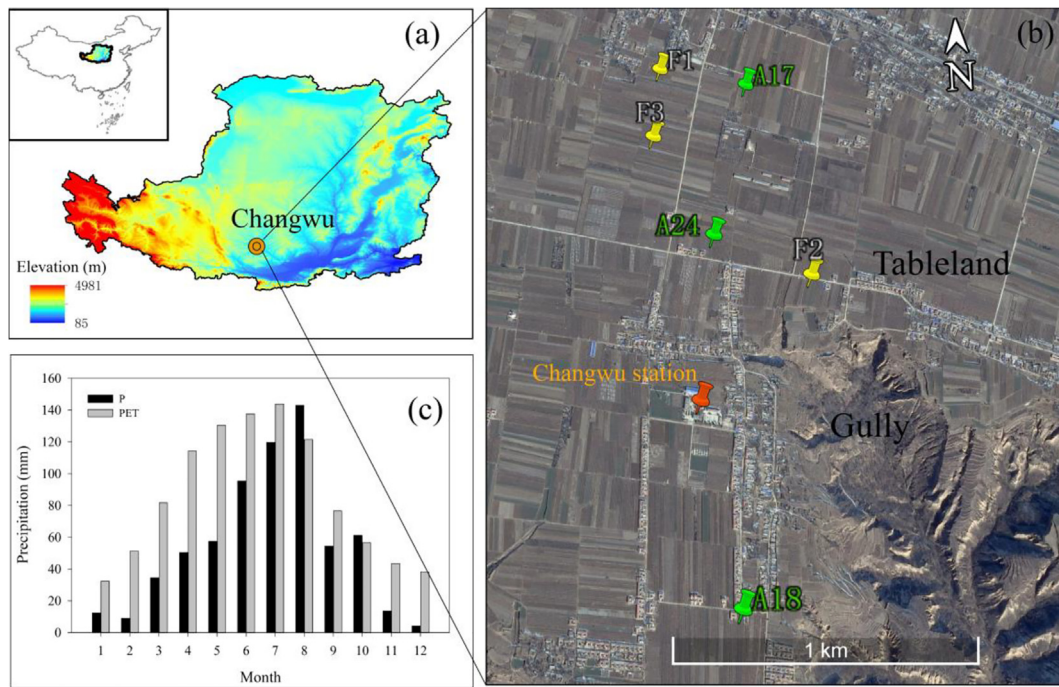


Fig. 1. Geographical location of the Changwu station and soil sampling sites (**a** and **b**). F and A in (**b**) represent long-term (> 100 years) farmlands (F1-3) and apple orchards (A17, A18, and A24; the number after the letter represents stand age of apple orchard, in year), respectively. Figure (**c**) showed the mean monthly precipitation (P) and potential evapotranspiration (PET) over the study period (2013–2018).

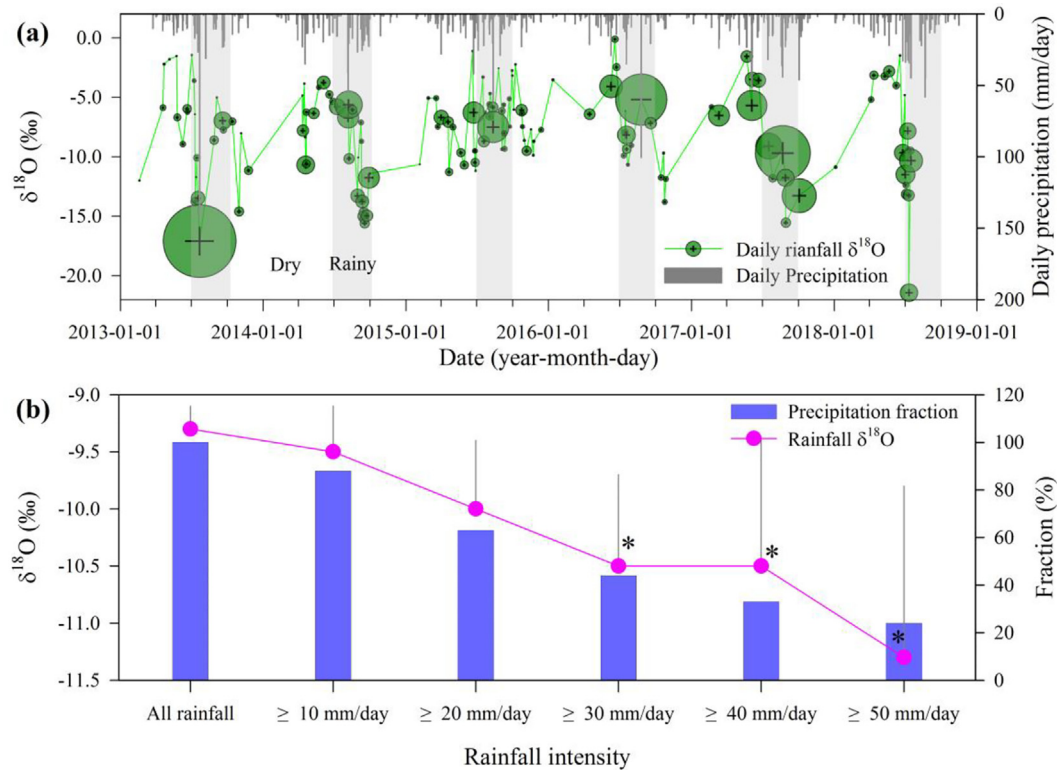


Fig. 2. Temporal variations of daily precipitation amount and $\delta^{18}\text{O}$ in precipitation (**a**). Circle size in (**a**) represents the daily precipitation amount. The white and gray area divide the dry (January to June and October to December) and rainy (July to September) seasons. Figure (**b**) showed $\delta^{18}\text{O}$ of different rainfall intensity and their ratios of cumulative amount to the annual precipitation. In (**b**), error bars represent one standard error; Statistically significant difference between $\delta^{18}\text{O}$ of different rainfall intensity and all rainfall are indicated with * ($t > 1.96$, $p < 0.05$).

Table 1
Basic information of the six soil profiles.

Profiles	Topography	Land use types and history	Sampling date	Shallow soil (0–4 m) $\delta^2\text{H}$	Shallow soil (0–4 m) $\delta^{18}\text{O}$	lc-excess	Deep soil (4–20 m) $\delta^2\text{H}$	Deep soil (4–20 m) $\delta^{18}\text{O}$	lc-excess
F1	Tableland	Farmland has a history of > 100 years.	10, June 2015	–68.0 (2.8) ^a	–9.2 (0.5)	–5.9 (1.0)	–72.1 (0.6)	–9.7 (0.1)	–5.7 (0.2)
F2	Tableland	Farmland has a history of > 100 years.	17, July 2018	–65.4 (4.9)	–8.8 (0.6)	–7.0 (0.5)	–69.7 (0.5)	–9.3 (0.1)	–7.5 (0.3)
F3	Tableland	Farmland has a history of > 100 years.	1, April 2017	–61.8 (1.8)	–8.5 (0.2)	–5.0 (0.6)	–71.9 (0.7)	–9.7 (0.1)	–6.4 (0.3)
A17	Tableland	17-year-old apple orchard, the previous land use is farmland.	10, June 2015	–72.9 (2.9)	–9.9 (0.5)	–5.8 (0.8)	–72.8 (0.5)	–9.7 (0.1)	–7.0 (0.2)
A18	Tableland	18-year-old apple orchard, the previous land use is farmland.	21, July 2016	–63.0 (1.2)	–8.7 (0.2)	–4.6 (0.5)	–73.5 (0.5)	–9.7 (0.5)	–8.0 (0.4)
A24	Tableland	24-year-old apple orchard, the previous land use is farmland.	21, July 2016	–61.7 (3.0)	–8.3 (0.5)	–6.9 (1.0)	–72.6 (0.5)	–9.9 (0.1)	–5.3 (0.4)

^a Number is the mean values and standard error (in bracket).

tritium units (1 TU = 1 H³/10¹⁸H) with the detection limit of 10.5 TU. This tritium profile has been used in our previous study to identify the water sources of apple trees in this orchard (Zhang et al., 2017).

2.4. Data analysis

2.4.1. Line-conditioned excess

We used the line-conditioned excess (lc-excess) approach (Landwehr and Coplen, 2006) to quantify the difference in the isotopic composition of soil waters from local precipitation, which by definition, has an lc-excess of zero:

$$lc - excess = \delta^2H - a\delta^{18}O - b \quad (2)$$

where a and b are slope and intercept of the Local Meteoric Water Line (LMWL), respectively. The LMWL is a linear regression that is derived based on the covariation of precipitation $\delta^2\text{H}$ and $\delta^{18}\text{O}$. The lc-excess approach distinguishes hydrological processes under chemical equilibrium (e.g. condensation of vapor), which generally has a positive lc-excess value, from hydrological processes that occur under disequilibrium (e.g. soil water evaporation), which generally has a negative lc-excess value (Sprenger et al., 2017). The LMWL at our site is based on the daily-based precipitation isotope data over eight hydrologic years (2005, 2010, and 2013–2018). The precipitation isotope data were fitted using the least-squares method, weighted by precipitation amount: $\delta^2\text{H} = (7.67 \pm 0.11) \delta^{18}\text{O} + (8.76 \pm 1.00)$, $n = 228$, $R^2 = 0.96$.

2.4.2. Identifying the soil water sources

Stable isotopes in water are well suitable for understanding hydrological processes because they are largely conservative tracers (Zimmermann et al., 1966). However, hydrological processes that occur under disequilibrium, such as soil water evaporation, produces strong kinetic isotope effects that leaves a isotopic characteristic of soil water that deviates its initial sources (i.e. precipitation) (Bowen et al., 2018). As a result, soil water isotope values have evolved along an evaporation line (EL) during the evaporation fractionation processes in the dual-isotope space, and back-correction along the EL to its intersection with the LMWL has been used to identify the isotopic composition of the initial sources from which the soil waters originated (Bowen et al., 2018; Evaristo et al., 2015). Based on these, we identified initial source water isotopic compositions for soil water by calculated the intersection of LMWL and soil water EL. The estimation of soil water EL slope was based on the Craig-Gordon model under a diffusion-controlled soil evaporation scenario (Benettin et al., 2018; Craig and Gordon, 1965; Gonfiantini, 1986):

$$Slope_{EL} = \frac{del_H}{del_O} \quad (3)$$

$$del_H(OR) = [hm * (\delta_P - \delta_A) - (1 + \delta_P * 10^{-3}) * (\epsilon_k + \epsilon/\alpha)] / (1 - hm + \epsilon_k * 10^{-3}) \quad (4)$$

where hm is the relative humidity [–], and δ_P and δ_A is the isotopic compositions of precipitation ($\delta^{18}\text{O} = -9.3\text{‰}$ and $\delta^2\text{H} = -62.5\text{‰}$ for this study) and atmosphere vapor [‰] (Gibson et al., 2008), respectively. The ϵ_k [‰] and α [–] is the kinetic (Benettin et al., 2018) and equilibrium fractionation factors (Horita and Wesolowski, 1994), respectively. The α was computed as ϵ ($\epsilon = (\alpha - 1)10^3$) [‰].

In this study, EL slope was estimated on daily basis using climatic data (temperature and relative humidity) over 1957–2018. The minimum, mean, and maximum temperature were all used to consider the uncertainty associated with the conditions under which evaporation occurs. This step is particularly important since evaporation conditions were largely variable with time. The calculated slopes ranged between 2.80 and 4.00, with a mean of 3.25 and standard deviation of 0.24

($n = 22,645$). We then used the long-term mean EL slope (3.25) to identify the isotopic compositions of initial source water for soil water in both shallow and deep soil water.

To identify the types of precipitation (events or seasons) associated with soil water recharge, we compared isotope values of initial soil water sources (i.e. intersection of EL and LMWL) with those of daily precipitation over eight years (2005, 2010, and 2013–2018). In specific, the types of precipitation were classified as follows. First, we divided precipitation isotope data into two seasons: rainy season (July to September) and dry season (January to June and October to December). Second, we classified precipitation isotope data into six categories based on the corresponding daily precipitation intensity: all rainfall; ≥ 10 mm/day rainfall; ≥ 20 mm/day rainfall; ≥ 30 mm/day rainfall; ≥ 40 mm/day rainfall, and ≥ 50 mm/day rainfall. The isotopic compositions of seasons and rainfall events with different intensities were calculated and weighted by precipitation amount, respectively.

2.4.3. Determination of soil water age

The radioactive tritium, which was released to atmosphere by intensive nuclear bomb testing and peaked in 1963, is often used as a time marker in hydrology (Li et al., 2019e; Lin and Wei, 2006). Assuming piston flow, the tritium peak in soil profile may present the 1963-precipitation tritium. Thus, soil water above/below the tritium peak depth represents water younger/older than 50 years, respectively. The determined age information was further used to constrain the soil water movement derived from stable isotopes.

2.4.4. Statistical analyses

For a given mean and standard error, Student's t test was used to analyze the difference between two means with unequal variances:

$$t = \frac{x - y}{\sqrt{\sigma_x^2 + \sigma_y^2}} \quad (3)$$

where x and y were the two mean values, and σ_x and σ_y were their respective standard errors. The statistically significant difference was indicated by $t > 1.96$ ($p < 0.05$).

3. Results

3.1. Stable isotopic compositions of precipitation

As $\delta^2\text{H}$ and $\delta^{18}\text{O}$ strongly covary, we only reported $\delta^{18}\text{O}$ values in the following sections. The $\delta^{18}\text{O}$ of daily-based precipitation showed a large variation, with values ranging from -21.4‰ to -0.1‰ (Fig. 2a). More negative (i.e. isotopically depleted) values were observed in the rainy season rather than the dry season. The amount-weighted $\delta^{18}\text{O}$ values in rainy and dry seasons varied from -99.6‰ to -43.3‰ and -49.8‰ to -30.3‰ , respectively (Table 2). The former had lower

isotopic values than the later, showing a clear seasonal variation. The amount-weighted $\delta^{18}\text{O}$ values were -10.9‰ for rainy season and -7.0‰ for dry season.

Based on all the precipitation isotope data (2005, 2010, and 2013–2018), the $\delta^{18}\text{O}$ values of all, ≥ 10 mm/day, ≥ 20 mm/day, ≥ 30 mm/day, ≥ 40 mm/day, and ≥ 50 mm/day rainfall events were -9.3‰ , -9.5‰ , -10.0‰ , -10.5‰ , -10.5‰ and -11.3‰ , respectively (Fig. 2b). The isotope values of large rainfall events (≥ 30 mm/day, ≥ 40 mm/day, and ≥ 50 mm/day rainfall events) were significantly negative than those of the long-term annual precipitation (i.e. all rainfall) ($p < 0.05$), suggesting the precipitation amount effect. As the cumulated amounts of large rainfall events account for 24 ~ 44% of the total rainfall amount, the variability in precipitation isotope data enables the identification of season and/or rainfall events recharging soil water.

3.2. Stable isotopic compositions of soil water

Stable isotopic compositions of soil water for all sites had similar vertical distribution, which varied in the shallow soils (0–4 m), but stabilized in soils below 4 m (Fig. 3a and b). The averaged $\delta^{18}\text{O}$ values ranged from -9.9‰ to -8.3‰ and the $\delta^2\text{H}$ values ranged from -72.9‰ to -61.7‰ for shallow soil water, while those for deep soil water are less variable (between -9.9‰ and -9.3‰ for $\delta^{18}\text{O}$, between -73.5‰ and -69.7‰ for $\delta^2\text{H}$) (Table 1). Furthermore, stable isotopic compositions beneath the farmland and apple orchard in shallow soils were more positive (i.e. isotopically enriched) than those in deep soils (student's t -test, $p < 0.05$) (Fig. 4b and c). However, lc-excess values in shallow soils were larger than those in deep soils (student's t -test, $p < 0.05$) (Fig. 4d). We noted that $\delta^{18}\text{O}$, $\delta^2\text{H}$, and lc-excess values in both shallow and deep soils under the apple orchard were similar to those under farmland (student's t -test, $p > 0.05$).

3.3. Soil water sources and ages

Since isotopic difference was observed between soil layers (i.e. shallow and deep) rather than land cover types (i.e. farmlands and apple orchards), we reported soil layers in what follows. Both shallow and deep soil water isotope plotted closely below the LMWL in the dual-isotope space (Fig. 4a), indicative of evaporation effects. We then back-correction along a EL to its intersection with the LMWL to offset the evaporation effects and to identify the isotopic composition of the initial sources (Fig. 5a). The isotopic compositions of the initial sources for shallow and deep soil water were ($\delta^{18}\text{O} = -10.4 \pm 1.3\text{‰}$ (average \pm standard deviation, thereafter), $\delta^2\text{H} = -70.8 \pm 10.2\text{‰}$) and ($\delta^{18}\text{O} = -11.2 \pm 0.5\text{‰}$, $\delta^2\text{H} = -77.4 \pm 3.8\text{‰}$), respectively. These values were different, and both isotopically depleted than that of the long-term amount-weighted precipitation ($\delta^{18}\text{O} = -9.3\text{‰}$,

Table 2
Amount-weighted mean values of stable isotopes in annual, rainy and dry season precipitation.

Year	$\delta^2\text{H}$ (‰)	Rainy season	Dry season	t value ^c	$\delta^{18}\text{O}$ (‰)	Rainy season	Dry season	t value
	Annual				Annual			
2005 ^a	-54.8 (4.7) ^b	-61.5 (6.6)	-46.5 (6.1)	1.67	-7.7 (0.6)	-8.9 (0.9)	-6.3 (0.6)	2.40
2010 ^a	-84.3 (7.0)	-99.6 (7.3)	-42.9 (7.8)	8.12	-12.3 (0.9)	-14.0 (0.9)	-7.6 (1.0)	4.76
2013 ^a	-80.0 (7.5)	-93.9 (9.5)	-49.8 (7.8)	3.59	-11.6 (1.0)	-13.2 (1.3)	-8.1 (1.0)	3.11
2014 ^a	-61.4 (5.7)	-73.1 (8.6)	-35.8 (5.8)	3.60	-9.5 (0.7)	-10.6 (1.1)	-7.1 (0.7)	2.68
2015 ^a	-48.2 (1.9)	-46.8 (2.7)	-49.2 (2.6)	0.64	-7.4 (0.3)	-6.8 (0.4)	-7.8 (0.4)	1.77
2016	-40.3 (5.1)	-43.3 (4.9)	-35.5 (9.6)	0.72	-6.6 (0.7)	-6.9 (0.6)	-6.0 (1.4)	0.59
2017	-57.4 (7.8)	-73.8 (5.3)	-42.6 (11.2)	2.52	-8.6 (1.0)	-10.4 (0.7)	-7.0 (1.5)	2.05
2018	-67.4 (9.6)	-87.7 (10.9)	-30.3 (8.9)	4.08	-9.9 (1.2)	-12.3 (1.3)	-5.5 (1.0)	4.15
All years	-62.5 (1.8)	-75.7 (3.1)	-42.7 (2.8)	7.90	-9.3 (0.2)	-10.9 (0.4)	-7.0 (0.4)	6.89

^a Data obtained from previous studies at the same study site (Cheng et al., 2014; Li et al., 2017b; Xiang et al., 2019).

^b Number in bracket is the standard error.

^c Student's t test was used to analyze the difference between rainy and dry season isotopes, where statistically significant difference are indicated with bold fonts ($t > 1.96$, $p < 0.05$).

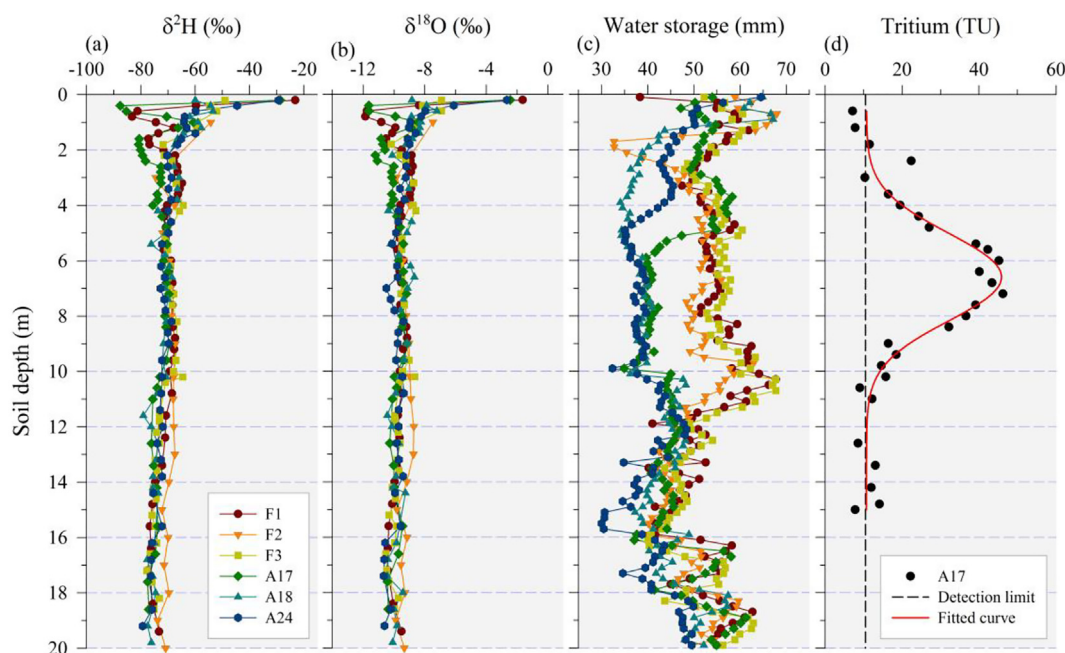


Fig. 3. Soil profiles of water stable isotopes (a and b), water storage (c), and water radioactive isotope (tritium; d). Figures (a)–(c) shared the sample legend presented in (a). Uppercase letters F and A represent farmland and apple orchard, respectively. The numbers after uppercase letter A are the stand age of apple orchards (in years). Tritium data in (d) are as reported in Zhang et al. (2017). The black dash line in (d) represents the limit of detection for the Liquid Scintillation Counter. The red tritium curve in (d) is fitted by the Gauss equation. (For interpretation of the references to colour in this figure legend, the reader is referred to the web version of this article.)

$\delta^2\text{H} = 62.5\text{‰}$) (Student *t*-test, $p < 0.05$).

To identify the types of precipitation recharging soil water, we compared soil water source isotopic compositions with that of the seasonal precipitation (Fig. 5a). While the shallow soil water source isotope value lied between the rainy ($\delta^{18}\text{O} = -10.9\text{‰}$, $\delta^2\text{H} = -75.7\text{‰}$) and dry seasons ($\delta^{18}\text{O} = -7.0\text{‰}$, $\delta^2\text{H} = -42.7\text{‰}$), deep soil water source isotope value was similar with the rainy season only. Comparing these source water isotope values to precipitation isotopic compositions with different rainfall intensities, the source water precipitation corresponded to an intensity of ≥ 20 and ≥ 30 mm/day for shallow and deep soils, respectively (Fig. 5b). The total amount of ≥ 20 and ≥ 30 mm/day rainfall events account to 63% and 44% of the total annual precipitation, respectively.

A clearly identifiable tritium peak at 6.6 m below the surface under the 17-year-old apple orchard (Fig. 3d), corresponded to the 1963 precipitation tritium abundance (Li et al., 2019e; Lin and Wei, 2006). This suggested that infiltrating water from 1963 precipitation has traveled approximately 6.6 m via piston flow over the past 54 years. By extension, soils deeper than 6.6 m were comprised of water older than ~ 50 years, while soils shallower than 6.6 m represented water younger than ~ 50 years.

3.4. Soil water storages

We noted that soil water storage at the depths of 4 to 12 m under the apple orchards was considerably lower than that of the farmlands (Fig. 3c). Because these sites are in close proximity to one another (< 1 km; Fig. 1b), subject to the same hydrometeorological and soil conditions at the study site, and the deep soil water content is invariable with time (Li et al., 2019c), the observed differences in deep soil water storage must result from land covers. Compared to farmland, deep soil water storage under apple orchards have an average deficit of 1027 mm, which is far greater than the annual mean precipitation (581 mm).

4. Discussion

4.1. Deep soil water recharge mechanisms in the Loess Plateau

Soil water stable isotopes were measured under different land covers (farmland and apple orchard) and at different time (Table 1). However, the water stable isotopes in deep soils (4–20 m) under farmlands and apple orchards were similar (Fig. 4). Shallow soil water isotopes may be affected by precipitation that occurred before soil sampling, and are not suitable for understanding the land use effects. Previous studies showed that deep soil water isotopic compositions were time-stable at our study site and other regions (Cheng et al., 2014; Sprenger et al., 2016). Our soil water tritium profile indicates that the deep soil water (> 7 m) is older than ~ 50 years (Fig. 3), but the apple orchards have been converted from farmlands for 24 years. It suggested that the stable isotopes below 7 m represents the long-term water balance of rainfall infiltration and evapotranspiration under farmlands earlier than ~ 50 years ago.

Soil water isotopes plotted closely below the LMWL (Fig. 4a), suggesting soil water had experienced in degrees of evaporation. Based on the theory-based approach, we identified the isotopic signature of shallow and deep soil water sources, which were both isotopically depleted than that of the long-term amount-weighted precipitation. Assumed that the atmospheric circulation and precipitation stable isotopes are in steady state (Tan et al., 2014; Liu et al., 2014; Liu et al., 2014), the modern precipitation isotope data (2005, 2010, and 2013–2018) has the representativeness of the long-term precipitation isotopic signatures at our site. Under such scenario, the above phenomenon can be attributed to the selective infiltration of seasonal precipitation or rainfall events (Jasechko et al., 2014; Li et al., 2018b). Thus, these suggested that: (i) Shallow and deep soil water originates from a portion of total precipitation; and (ii) More isotopically depleted precipitation is needed to deep soil water recharge compared to shallow soil.

Comparing these isotopic signatures of soil water sources with precipitation isotope data (Fig. 5), we found that: (i) Rainfall events in

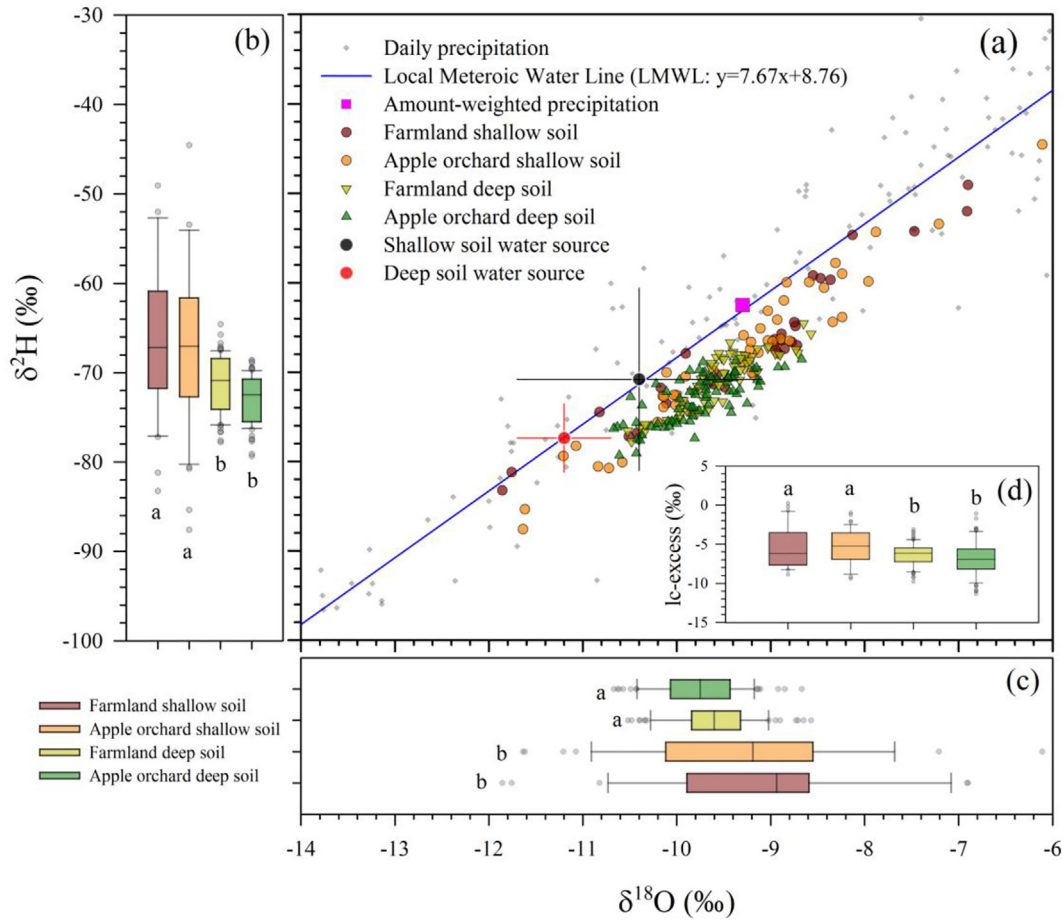


Fig. 4. Stable isotopic compositions of precipitation and soil water at the study site. Figure (a) showed stable isotopic compositions of soil water within the shallow (0–4 m) and deep (4–20 m) soils under farmland and apple orchard in the dual-isotope space. Error bars in (a) represent one standard deviation. Figure (b)–(d) showed the Box plot (10th, 25th, 50th, 75th, and 90th) of soil water $\delta^2\text{H}$, $\delta^{18}\text{O}$, and line-conditioned excess (lc-excess), respectively. Different letters next to the box plot in (b)–(d) indicate significant differences in isotope data according to the post hoc Tukey test ($\alpha = 0.05$).

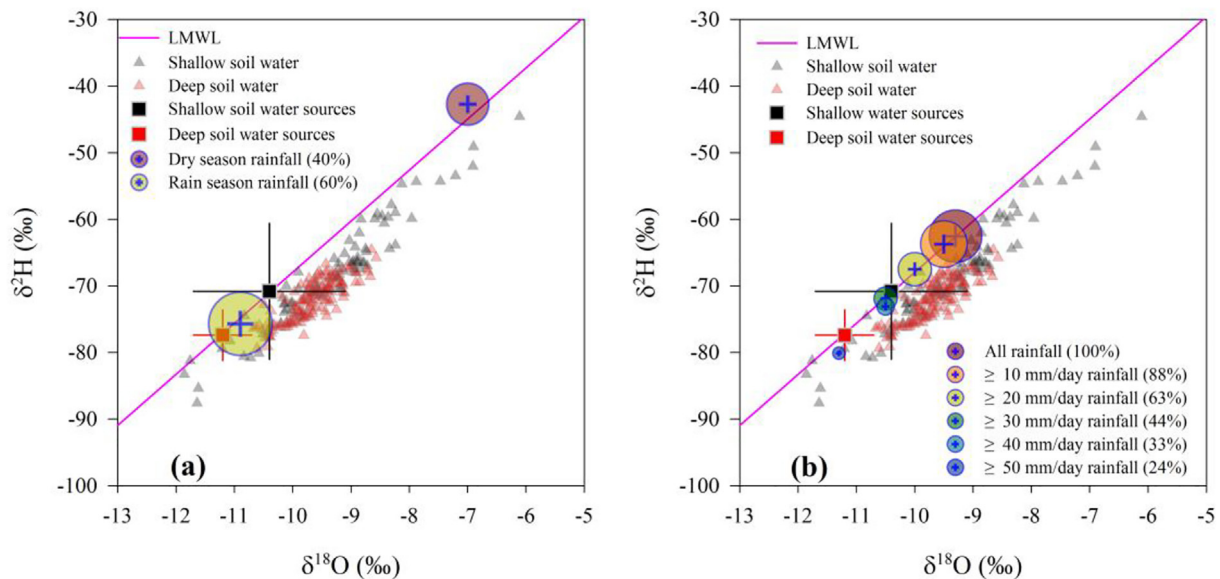


Fig. 5. Stable isotopic compositions of precipitation and soil water sources at the study site. Figure (a) showed the relationships between seasonal precipitation and water sources of shallow (0–4 m) and deep (4–20 m) soils. Figure (b) showed the relationship between different rainfall intensity and water sources of shallow and deep soils. In (a) and (b), error bars in (b) represent one standard error; LMWL represents the Local Meteoric Water Line ($\delta^2\text{H} = 7.67 \delta^{18}\text{O} + 8.76$); size of bubbles and values represents the fraction (expressed in %) of total seasonal or event precipitation amount to the annual precipitation.

both rainy and dry seasons could recharge shallow soils, whereas deep soil water only originated from rainy season precipitation; and (ii) Most rainfall events (≥ 20 mm/day; 63% of the annual precipitation) can recharge shallow soil water, but only high-intensity rainfall events (≥ 30 mm/day; 24 ~ 44% of the annual precipitation) are the source of deep soil water. Therefore, we conclude that water in deep soils mainly originated from episodic, high-intensity rainfall events that fell during the rainy season. This is not surprising because monthly precipitation during the rainy season, especially in August and September, is equal to or greater than the potential evapotranspiration over 2013–2018 (Fig. 1c). This indicates that a portion of surplus precipitation was available for recharge of deep soil water. In addition, the precipitation infiltration depth was closely related to rainfall amount and intensity, that is, the larger the rainfall event, the greater the infiltration depth (Jin et al., 2018; Wiekenkamp et al., 2016). At our study site, which is characterized by a monsoon climate, more than half of annual precipitation occurs in the rainy season as short-duration heavy rainfall, and most of these events are over the threshold rainfall intensity (30 mm/day) (Fig. 2). These high-intensity events would have activated the large pores in shallow soils (Beven and Germann, 2013), thereby enabling a mechanism that transmits infiltration water to deeper parts of the soil profile. Our isotope-based results are consistent with current findings from soil water observation (Jin et al., 2018; Liu et al., 2010) and modeling work (Shao et al., 2018a), which underlined the importance of high-intense rainfall, or rainy season, or extreme wet year for deep soil water recharge.

Soil water tritium indicated that the age of water in deep soils (> 6 m) were older than ~50 years. As the precipitation infiltration at CLP is predominantly piston flow (Li et al., 2018a; Li et al., 2019e; Lin and Wei, 2006; Xiang et al., 2019), the precipitation during the life-span of apple orchards (< 24 years) were not likely to recharge deep soil water. Characterized by a sub-humid climate (aridity index is 0.65), infiltrated precipitation may be rapidly evaporated and transpired within the shallow soils at our study site. Meanwhile, as the higher root water uptake of apple trees than that of farmland (i.e. winter maize or summer corn) (Wang et al., 2011), this thereby resulted in considerably smaller deep soil water stores beneath the apple orchards than nearby farmland. This observation was referred to as “one-off” root water uptake by Li et al. (2019c) to distinguish this mode of root water uptake from the type that is characteristic of humid regions (Rempe and Dietrich, 2018; Salve et al., 2012). From the above, water stable and radioactive isotopes combined reveal that the deep soil water originated from episodic, high-intensity rainfall events, but the recharging water predated the ages of apple trees that presently dot these landscapes.

These findings have important implications for the sustainable management of soil water resources in the CLP. In this region, the growing season of traditional shallow-rooted crops (e.g. winter wheat) is from November to April of the following year, but deep-rooted trees have a growing season from April to September (Wang and Wang, 2018). This coincides with the deep soil water recharge period. Moreover, infiltration water from high-intensity rainfall events rarely makes it below the rooting zone of trees because of low infiltration rate (Huang et al., 2013) and well-developed root systems (Li et al., 2019b). Ecohydrologically, the conversion of farmland or grassland to forestland with developed roots could reduce deep soil water recharge and further decrease potential groundwater recharge at CLP (Huang et al., 2018; Zhang et al., 2018). Thus, to ensure the sustainability of revegetation in this region, appropriate measures need to be developed to balance water supply and ecological water consumption in deep soils.

4.2. Tritium as a constraint to stable water isotope interpretations

Determining the ages of soil water is important for the interpretation of soil and hydrological processes (Sprenger et al., 2019). In addition to sources and partitioning, water stable isotopes are suitable for

characterizing the ages of water with younger than a few years in shallow vadose zone or outflows within catchment by using peak displacement method (Birkel et al., 2014). However, this is a problem in deep vadose and saturated zone hydrology because the subsurface water processes, dynamics, and feedbacks are mediated by the soil (Brooks et al., 2015). Conversely, tritium has been widely used to determine the age of water up to several decades in the subsurface (Gleeson et al., 2016; Morgenstern et al., 2010). Our work here demonstrates that soil water tritium can serve as a constraint to water stable isotope interpretations in places where the tritium method is viable (Allison and Hughes, 1975; Li and Si, 2018; O'Brien et al., 1996; Si and de Jong, 2007). If it were not for our tritium measurements, constraints on the relative ages of water at different parts of deep soils would not have been possible. The clear demarcation between water older and younger than ~50 years at > 6.6 m and < 6.6 m depths, respectively, was made possible because of tritium. Altogether, the tritium-derived age information complements the water stable isotope interpretations, thereby, advancing our understanding of water flow and transport in these deep loess deposits in China.

5. Conclusions

We sampled six 20-m-deep soil profiles for water stable ($\delta^2\text{H}$ and $\delta^{18}\text{O}$) and radioactive (^3H , tritium) isotopes to determine the sources of soil water under contrasting farmland and apple orchard in CLP. We found that soil water tritium concentrations may serve as a powerful time (water age) and space (depth distribution) compensate for stable water isotope interpretations. Stable isotopes suggested that deep soil water mainly originated from rainy season precipitation, and a speculated threshold rainfall intensity of ≥ 30 mm/day. However, the soil water tritium indicated that deep soil water is much older, and impossible recharged by precipitation over the life-span of apple trees. These insights, gathered from the combined use of water stable and radioactive isotopic tracers, support the conclusion that recharge of water to deeper soils was less frequent in time in the CLP.

Declaration of Competing Interest

The authors declare that they have no known competing financial interests or personal relationships that could have appeared to influence the work reported in this paper.

Acknowledgments

This work was jointly funded by the Strategic Priority Research Program of Chinese Academy of Sciences (XDB40020200), Natural Science Foundation of China (51179161) and Natural Science Foundation of Shaanxi Province (2018JZ4001). The constructive comments from two anonymous referees are greatly appreciated.

References

- Allen, S.T., Kirchner, J.W., Braun, S., Siegwolf, R.T.W., Goldsmith, G.R., 2019. Seasonal origins of soil water used by trees. *Hydrol. Earth Syst. Sci.* 23 (2), 1199–1210. <https://doi.org/10.5194/hess-23-1199-2019>.
- Allison, G.B., Hughes, M.W., 1975. The use of environmental tritium to estimate recharge to a South-Australian aquifer. *J. Hydrol.* 26 (3–4), 245–254. [https://doi.org/10.1016/0022-1694\(75\)90006-2](https://doi.org/10.1016/0022-1694(75)90006-2).
- Benettin, P., Volkmann, T.H.M., von Freyberg, J., Frentress, J., Penna, D., Dawson, T.E., Kirchner, J., 2018. Effects of climatic seasonality on the isotopic composition of evaporating soil waters. *Hydrol. Earth Syst. Sci.* 22 (5), 2881–2890. <https://doi.org/10.5194/hess-22-2881-2018>.
- Berry, Z.C., Evaristo, J., Moore, G., Poca, M., Steppe, K., Verrot, L., Asbjornsen, H., Borma, L.S., Bretfeld, M., Herve-Fernandez, P., Seyfried, M., Schwendenmann, L., Sinacore, K., De Wispelaere, L., McDonnell, J., 2018. The two water worlds hypothesis: addressing multiple working hypotheses and proposing a way forward. *Ecohydrology* 11 (3), e1843. <https://doi.org/10.1002/Eco.1843>.
- Beven, K., Germann, P., 2013. Macropores and water flow in soils revisited. *Water Resour. Res.* 49 (6), 3071–3092. <https://doi.org/10.1002/wrcr.20156>.
- Birkel, C., Soulsby, C., Tetzlaff, D., 2014. Developing a consistent process-based

- conceptualization of catchment functioning using measurements of internal state variables. *Water Resour. Res.* 50 (4), 3481–3501. <https://doi.org/10.1002/2013WR014925>.
- Bowen, G., 2015. Hydrology: The diversified economics of soil water. *Nature* 525 (7567), 43–44. <https://doi.org/10.1038/525043a>.
- Bowen, G.J., Putman, A., Brooks, J.R., Bowling, D.R., Oerter, E.J., Good, S.P., 2018. Inferring the source of evaporated waters using stable H and O isotopes. *Oecologia* 187 (4), 1025–1039. <https://doi.org/10.1007/s00442-018-4192-5>.
- Brantley, S.L., McDowell, W.H., Dietrich, W.E., White, T.S., Kumar, P., Anderson, S.P., Chorover, J., Lohse, K.A., Bales, R.C., Richter, D.D., Grant, G., Gaillardet, J., 2017. Designing a network of critical zone observatories to explore the living skin of the terrestrial Earth. *Earth Surf. Dyn.* 5 (4), 841–860. <https://doi.org/10.5194/esurf-5-841-2017>.
- Brooks, J.P., 2015. Water, bound and mobile. *Science* 349 (6244), 138–139. <https://doi.org/10.1126/science.aac4742>.
- Brooks, J.R., Barnard, H.R., Coulombe, R., McDonnell, J.J., 2010. Ecohydrologic separation of water between trees and streams in a Mediterranean climate. *Nat. Geosci.* 3 (2), 100–104. <https://doi.org/10.1038/NGEO722>.
- Brooks, P.D., Chorover, J., Fan, Y., Godsey, S.E., Maxwell, R.M., McNamara, J.P., Tague, C., 2015. Hydrological partitioning in the critical zone: recent advances and opportunities for developing transferable understanding of water cycle dynamics. *Water Resour. Res.* 51 (9), 6973–6987. <https://doi.org/10.1002/2015WR017039>.
- Cheng, L.P., Liu, W.Z., Li, Z., Chen, J., 2014. Study of soil water movement and groundwater recharge for the loess tableland using environmental tracers. *Trans. ASABE* 57 (1), 23–30. <https://doi.org/10.13031/trans.56.10017>.
- Craig, H., 1961. Isotopic variations in meteoric waters. *Science* 133 (3465), 1702–1703. <https://doi.org/10.1126/science.133.3465.1702>.
- Craig, H., Gordon, L.I., 1965. Deuterium and oxygen 18 variations in the ocean and marine atmosphere. In: Tongiorgi, E. (Ed.), *Stable Isotopes in Oceanographic Studies and Paleotemperatures*, Spoleto, Italy. *Stable Isotopes in Oceanographic Studies and Paleotemperatures*, Spoleto, Italy, pp. 9–130.
- Evaristo, J., Jasechko, S., McDonnell, J.J., 2015. Global separation of plant transpiration from groundwater and streamflow. *Nature* 525 (7567), 91–94. <https://doi.org/10.1038/nature14983>.
- Evaristo, J., McDonnell, J.J., 2019. Global analysis of streamflow response to forest management. *Nature* 570 (7762), 455–461. <https://doi.org/10.1038/s41586-019-1306-0>.
- Evaristo, J., McDonnell, J.J., Scholl, M.A., Bruijnzeel, L.A., Chun, K.P., 2016. Insights into plant water uptake from xylem-water isotope measurements in two tropical catchments with contrasting moisture conditions. *Hydrol. Process.* 30 (18), 3210–3227. <https://doi.org/10.1002/hyp.10841>.
- Feng, X.M., Fu, B.J., Piao, S., Wang, S.H., Ciais, P., Zeng, Z.Z., Lu, Y.H., Zeng, Y., Li, Y., Jiang, X.H., Wu, B.F., 2016. Revegetation in China's Loess Plateau is approaching sustainable water resource limits. *Nat. Clim. Change* 6 (11), 1019–1022. <https://doi.org/10.1038/Nclimate3092>.
- Fu, B.J., Wang, S., Liu, Y., Liu, J.B., Liang, W., Miao, C.Y., 2017. Hydrogeomorphic ecosystem responses to natural and anthropogenic changes in the Loess Plateau of China. *Annu. Rev. Earth Planet. Sci.* 45, 223–243. <https://doi.org/10.1146/annurev-earth-063016-020552>.
- Giardina, F., Konings, A.G., Kennedy, D., Alemohammad, S.H., Oliveira, R.S., Uriarte, M., Gentile, P., 2018. Tall Amazonian forests are less sensitive to precipitation variability. *Nat. Geosci.* 11 (6), 405–+. <https://doi.org/10.1038/s41561-018-0133-5>.
- Gibson, J.J., Birks, S.J., Edwards, T.W.D., 2008. Global prediction of δ_A and δ^2H - $\delta^{18}O$ evaporation slopes for lakes and soil water accounting for seasonality. *Global Biogeochem. Cy.* 22 (2), GB2031. <https://doi.org/10.1029/2007gb002997>.
- Gleeson, T., Befus, K.M., Jasechko, S., Luijendijk, E., Cardenas, M.B., 2016. The global volume and distribution of modern groundwater. *Nat. Geosci.* 9 (2), 161. <https://doi.org/10.1038/NGEO2590>.
- Gonfiantini, R., 1986. Environmental isotopes in lake studies, in: *The Terrestrial Environment*. In: Fritz, P., Fontes, J.C. (Eds.), *Handbook of Environmental Isotope Geochemistry*. Elsevier, Amsterdam, pp. 113–168.
- Good, S.P., Noone, D., Bowen, G., 2015. Water resources. Hydrologic connectivity constrains partitioning of global terrestrial water fluxes. *Science* 349 (6244), 175–177. <https://doi.org/10.1126/science.aaa5931>.
- Horita, J., Wesolowski, D.J., 1994. Liquid-vapor fractionation of oxygen and hydrogen isotopes of water from the freezing to the critical-temperature. *Geochim. Cosmochim. Acta* 58 (16), 3425–3437. [https://doi.org/10.1016/0016-7037\(94\)90096-5](https://doi.org/10.1016/0016-7037(94)90096-5).
- Huang, T.M., Pang, Z.H., Edmunds, W.M., 2013. Soil profile evolution following land-use change: implications for groundwater quantity and quality. *Hydrol. Process.* 27 (8), 1238–1252. <https://doi.org/10.1002/hyp.9302>.
- Huang, Y.N., Chang, Q.R., Li, Z., 2018. Land use change impacts on the amount and quality of recharge water in the loess tablelands of China. *Sci. Total Environ.* 628–629, 443–452. <https://doi.org/10.1016/j.scitotenv.2018.02.076>.
- Jasechko, S., Birks, S.J., Gleeson, T., Wada, Y., Fawcett, P.J., Sharp, Z.D., McDonnell, J.J., Welker, J.M., 2014. The pronounced seasonality of global groundwater recharge. *Water Resour. Res.* 50 (11), 8845–8867. <https://doi.org/10.1002/2014WR015809>.
- Jia, X.X., Shao, M.A., Zhu, Y.J., Luo, Y., 2017. Soil moisture decline due to afforestation across the Loess Plateau, China. *J. Hydrol.* 546, 113–122. <https://doi.org/10.1016/j.jhydrol.2017.01.011>.
- Jin, Z., Guo, L., Lin, H., Wang, Y.Q., Yu, Y.L., Chu, G.C., Zhang, J., 2018. Soil moisture response to rainfall on the Chinese Loess Plateau after a long-term vegetation rehabilitation. *Hydrol. Process.* 32 (12), 1738–1754. <https://doi.org/10.1002/hyp.13143>.
- Landwehr, J.M., Coplen, T.B., 2006. Line-conditioned excess: a new method for characterizing stable hydrogen and oxygen isotope ratios in hydrologic systems. In: *International Conference on Isotopes in Environmental Studies*. IAEA, Vienna, pp. 132–135.
- Li, B.B., Wang, Y.Q., Hill, R.L., Li, Z., 2019a. Effects of apple orchards converted from farmlands on soil water balance in the deep loess deposits based on HYDRUS-1D model. *Agric. Ecosyst. Environ.* 285, 106645. <https://doi.org/10.1016/j.agee.2019.106645>.
- Li, H., Si, B.C., Li, M., 2018a. Rooting depth controls potential groundwater recharge on hillslopes. *J. Hydrol.* 564, 164–174. <https://doi.org/10.1016/j.jhydrol.2018.07.002>.
- Li, H.J., Si, B.C., Ma, X.J., Wu, P.T., 2019b. Deep soil water extraction by apple sequesters organic carbon via root biomass rather than altering soil organic carbon content. *Sci. Total Environ.* 670, 662–671. <https://doi.org/10.1016/j.scitotenv.2019.03.267>.
- Li, H.J., Si, B.C., Wu, P.T., McDonnell, J.J., 2019c. Water mining from the deep critical zone by apple trees growing on loess. *Hydrol. Process.* 33 (2), 320–327. <https://doi.org/10.1002/hyp.13346>.
- Li, J., Pang, Z., Kong, Y., Wang, S., Bai, G., Zhao, H., Zhou, D., Sun, F., Yang, Z., 2018b. Groundwater isotopes biased toward heavy rainfall events and implications on the local meteoric water line. *J. Geophys. Res. Atmos.* 123 (11), 6259–6266. <https://doi.org/10.1029/2018jd028413>.
- Li, J.J., Peng, S.Z., Li, Z., 2017a. Detecting and attributing vegetation changes on China's Loess Plateau. *Agric. Forest Meteorol.* 247, 260–270. <https://doi.org/10.1016/j.agrformet.2017.08.005>.
- Li, Z., Coles, A.E., Xiao, J., 2019d. Groundwater and streamflow sources in China's Loess Plateau on catchment scale. *Catena* 181, 104075. <https://doi.org/10.1016/J.Catena.2019.104075>.
- Li, Z., Jasechko, S., Si, B.C., 2019e. Uncertainties in tritium mass balance models for groundwater recharge estimation. *J. Hydrol.* 571, 150–158. <https://doi.org/10.1016/j.jhydrol.2019.01.030>.
- Li, Z., Lin, X., Xiang, W., Chen, X., Huang, T., 2017b. Stable isotope tracing of headwater sources in a river on China's Loess Plateau. *Hydrol. Sci. J.* 62 (13), 2150–2159. <https://doi.org/10.1080/02626667.2017.1368519>.
- Li, Z., Si, B.C., 2018. Reconstructed precipitation tritium leads to overestimated groundwater recharge. *J. Geophys. Res. Atmos.* 123 (17), 9858–9867. <https://doi.org/10.1029/2018JD028405>.
- Lin, R.F., Wei, K.Q., 2006. Tritium profiles of pore water in the Chinese loess unsaturated zone: Implications for estimation of groundwater recharge. *J. Hydrol.* 328 (1–2), 192–199. <https://doi.org/10.1016/j.jhydrol.2005.12.010>.
- Liu, Z.Y., Wen, X.Y., Brady, E.C., Otto-Bliesner, B., Yu, G., Lu, H.Y., Cheng, H., Wang, Y.J., Zheng, W.P., Ding, Y.H., Edwards, R.L., Cheng, J., Liu, W., Yang, H., 2014. Chinese cave records and the East Asia Summer Monsoon. *Quat. Sci. Rev.* 83, 115–128. <https://doi.org/10.1016/j.quascirev.2013.10.021>.
- Liu, W.Z., Zhang, X.C., Dang, T.H., Zhu, O.Y., Li, Z., Wang, J., Wang, R., Gao, C.Q., 2010. Soil water dynamics and deep soil recharge in a record wet year in the southern Loess Plateau of China. *Agric. Water Manage.* 97 (8), 1133–1138. <https://doi.org/10.1016/j.agwat.2010.01.001>.
- Liu, J.R., Song, X.F., Yuan, G.F., Sun, X.M., Yang, L.H., 2014. Stable isotopic compositions of precipitation in China. *Tellus B* 66 (1), 1–17. <https://doi.org/10.3402/Tellusb.v66.22567>.
- Lu, Y.W., Si, B.C., Li, H.J., Biswas, A., 2019. Elucidating controls of the variability of deep soil bulk density. *Geoderma* 348, 146–157. <https://doi.org/10.1016/j.geoderma.2019.04.033>.
- McCutcheon, R.J., McNamara, J.P., Kohn, M.J., Evans, S.L., 2017. An evaluation of the ecohydrological separation hypothesis in a semiarid catchment. *Hydrol. Process.* 31 (4), 783–799. <https://doi.org/10.1002/hyp.11052>.
- McGuire, K.J., McDonnell, J.J., 2015. Tracer advances in catchment hydrology. *Hydrol. Process.* 29 (25), 5135–5138. <https://doi.org/10.1002/hyp.10740>.
- Morgenstern, U., Stewart, M.K., Stenger, R., 2010. Dating of streamwater using tritium in a post nuclear bomb pulse world: continuous variation of mean transit time with streamflow. *Hydrol. Earth Syst. Sci.* 14 (11), 2289–2301. <https://doi.org/10.5194/hess-14-2289-2010>.
- Nepstad, D.C., Decarvalho, C.R., Davidson, E.A., Jipp, P.H., Lefebvre, P.A., Negreiros, G.H., Dasilva, E.D., Stone, T.A., Trumbore, S.E., Vieira, S., 1994. The role of deep roots in the hydrological and carbon cycles of amazonian forests and pastures. *Nature* 372 (6507), 666–669. <https://doi.org/10.1038/372666a0>.
- O'Brien, R., Keller, C.K., Smith, J.L., 1996. Multiple tracers of shallow ground-water flow and recharge in hilly loess. *Ground Water* 34 (4), 675–682. <https://doi.org/10.1111/j.1745-6584.1996.tb02055.x>.
- Orlowski, N., Breuer, L., McDonnell, J.J., 2016. Critical issues with cryogenic extraction of soil water for stable isotope analysis. *Ecohydrology* 9 (1), 3–10. <https://doi.org/10.1002/eco.1722>.
- Peng, S.Z., Li, Z., 2018. Incorporation of potential natural vegetation into revegetation programmes for sustainable land management. *Land Degrad. Dev.* 29 (10), 3503–3511. <https://doi.org/10.1002/ldr.3124>.
- Penna, D., Hopp, L., Scandellari, F., Allen, S.T., Benettin, P., Beyer, M., Geris, J., Klaus, J., Marshall, J.D., Schwendenmann, L., Volkmann, T.H.M., von Freyberg, J., Amin, A., Ceperley, N., Engel, M., Frentress, J., Giambastiani, Y., McDonnell, J.J., Zuecco, G., Llorens, P., Siegwolf, R.T.W., Dawson, T.E., Kirchner, J.W., 2018. Ideas and perspectives: tracing terrestrial ecosystem water fluxes using hydrogen and oxygen stable isotopes – challenges and opportunities from an interdisciplinary perspective. *Biogeosciences* 15 (21), 6399–6415. <https://doi.org/10.5194/bg-15-6399-2018>.
- Rempe, D.M., Dietrich, W.E., 2018. Direct observations of rock moisture, a hidden component of the hydrologic cycle. *Proc. Natl. Acad. Sci. USA* 115 (11), 2664–2669. <https://doi.org/10.1073/pnas.1800141115>.
- Salve, R., Rempe, D.M., Dietrich, W.E., 2012. Rain, rock moisture dynamics, and the rapid response of perched groundwater in weathered, fractured argillite underlying a steep hillslope. *Water Resour. Res.* 48. <https://doi.org/10.1029/2012wr012583>.
- Shao, J., Si, B.C., Jin, J.M., 2018a. Extreme precipitation years and their occurrence frequency regulate long-term groundwater recharge and transit time. *Vadose Zone J.*

- 17 (1). <https://doi.org/10.2136/Vzj2018.04.0093>.
- Shao, M.A., Wang, Y.Q., Xia, Y.Q., Jia, X.X., 2018b. Soil drought and water carrying capacity for vegetation in the critical zone of the loess plateau: a review. *Vadose Zone J.* 17 (1), 8. <https://doi.org/10.2136/Vzj2017.04.0077>.
- Si, B.C., de Jong, E., 2007. Determining long-term (decadal) deep drainage rate using multiple tracers. *J. Environ. Qual.* 36 (6), 1686–1694. <https://doi.org/10.2134/jeq2007.0029>.
- Sprenger, M., Leistert, H., Gimbel, K., Weiler, M., 2016. Illuminating hydrological processes at the soil-vegetation-atmosphere interface with water stable isotopes. *Rev. Geophys.* 54 (3), 674–704. <https://doi.org/10.1002/2015RG000515>.
- Sprenger, M., Stumpp, C., Weiler, M., Aeschbach, W., Allen, S.T., Benettin, P., Dubbert, M., Hartmann, A., Hrachowitz, M., Kirchner, J.W., McDonnell, J.J., Orlowski, N., Penna, D., Pfahl, S., Rinderer, M., Rodriguez, N., Schmidt, M., Werner, C., 2019. The demographics of water: a review of water ages in the critical zone. *Rev. Geophys.* <https://doi.org/10.1029/2018rg000633>.
- Sprenger, M., Tetzlaff, D., Tunaley, C., Dick, J., Soulsby, C., 2017. Evaporation fractionation in a peatland drainage network affects stream water isotope composition. *Water Resour. Res.* 53 (1), 851–866. <https://doi.org/10.1002/2016WR019258>.
- Stewart, M.K., Morgenstern, U., McDonnell, J.J., 2010. Truncation of stream residence time: how the use of stable isotopes has skewed our concept of streamwater age and origin. *Hydrol. Process.* 24 (12), 1646–1659. <https://doi.org/10.1002/hyp.7576>.
- Tan, L.C., An, Z.S., Huh, C.A., Cai, Y.J., Shen, C.C., Shiau, L.J., Yan, L.B., Cheng, H., Edwards, R.L., 2014. Cyclic precipitation variation on the western Loess Plateau of China during the past four centuries. *Sci. Rep.* 4, 6381. <https://doi.org/10.1038/srep06381>.
- Wang, D., Wang, L., 2018. Canopy interception of apple orchards should not be ignored when assessing evapotranspiration partitioning on the Loess Plateau in China. *Hydrol. Process.* 33 (3), 372–382. <https://doi.org/10.1002/hyp.13330>.
- Wang, Y.Q., Hu, W., Zhu, Y.J., Shao, M.A., Xiao, S., Zhang, C.C., 2015. Vertical distribution and temporal stability of soil water in 21-m profiles under different land uses on the Loess Plateau in China. *J. Hydrol.* 527, 543–554. <https://doi.org/10.1016/j.jhydrol.2015.05.010>.
- Wang, Y.Q., Shao, M.A., Zhu, Y.J., Liu, Z.P., 2011. Impacts of land use and plant characteristics on dried soil layers in different climatic regions on the Loess Plateau of China. *Agric. Forest Meteorol.* 151 (4), 437–448. <https://doi.org/10.1016/j.agrformet.2010.11.016>.
- Wiekenkamp, I., Huisman, J.A., Bogaen, H.R., Lin, H.S., Vereecken, H., 2016. Spatial and temporal occurrence of preferential flow in a forested headwater catchment. *J. Hydrol.* 534, 139–149. <https://doi.org/10.1016/j.jhydrol.2015.12.050>.
- Xiang, W., Si, B.C., Biswas, A., Li, Z., 2019. Quantifying dual recharge mechanisms in deep unsaturated zone of Chinese Loess Plateau using stable isotopes. *Geoderma* 337, 773–781. <https://doi.org/10.1016/j.geoderma.2018.10.006>.
- Xu, X., Guan, H., Skrzypek, G., Simmons, C.T., 2019. Root-zone moisture replenishment in a native vegetated catchment under Mediterranean climate. *Hydrol. Process.* 33 (18), 2394–2407. <https://doi.org/10.1002/hyp.13475>.
- Yang, F.T., Feng, Z.M., Wang, H.M., Dai, X.Q., Fu, X.L., 2017. Deep soil water extraction helps to drought avoidance but shallow soil water uptake during dry season controls the inter-annual variation in tree growth in four subtropical plantations. *Agric. Forest Meteorol.* 234, 106–114. <https://doi.org/10.1016/j.agrformet.2016.12.020>.
- Yang, L., Wei, W., Chen, L.D., Mo, B.R., 2012. Response of deep soil moisture to land use and afforestation in the semi-arid Loess Plateau, China. *J. Hydrol.* 475, 111–122. <https://doi.org/10.1016/j.jhydrol.2012.09.041>.
- Zhang, Z.Q., Evaristo, J., Li, Z., Si, B.C., McDonnell, J.J., 2017. Tritium analysis shows apple trees may be transpiring water several decades old. *Hydrol. Process.* 31 (5), 1196–1201. <https://doi.org/10.1002/hyp.11108>.
- Zhang, Z.Q., Li, M., Si, B.C., Feng, H., 2018. Deep rooted apple trees decrease groundwater recharge in the highland region of the Loess Plateau, China. *Sci. Total Environ.* 622–623, 584–593. <https://doi.org/10.1016/j.scitotenv.2017.11.230>.
- Zhu, X.M., Li, Y.S., Peng, X.L., Zhang, S.G., 1983. Soils of the loess region in China. *Geoderma* 29 (3), 237–255. [https://doi.org/10.1016/0016-7061\(83\)90090-3](https://doi.org/10.1016/0016-7061(83)90090-3).
- Zhu, Y.J., Jia, X.X., Shao, M.A., 2018. Loess thickness variations across the Loess Plateau of China. *Surv. Geophys.* 39 (4), 715–727. <https://doi.org/10.1007/s10712-018-9462-6>.
- Zimmermann, U., Munnich, K.O., Roether, W., Kreutz, W., Schubach, K., Siegel, O., 1966. Tracers determine movement of soil moisture and evapotranspiration. *Science* 152 (3720), 346–347. <https://doi.org/10.1126/science.152.3720.346>.
- Zunzunegui, M., Boutaleb, S., Diaz Barradas, M.C., Esquivias, M.P., Valera, J., Jauregui, J., Tagma, T., Ain-Lhout, F., 2018. Reliance on deep soil water in the tree species *Argania spinosa*. *Tree Physiol.* 38 (5), 678–689. <https://doi.org/10.1093/treephys/tpx152>.